molecule and cyclization occur either in concert or in rapid sequence, for bond rotation within the conjugated ring-opened enol would result in loss of stereoselectivity and a mixture of diastereomeric products would result. Hydrogen bonding with the carboxylate oxygen is likely important in retaining the closed structure for the ring-opened conjugated alcohol chain.

Conclusions

The coordination chemistry of the Phenox quinone imine ligand differs from the complexes of ruthenium formed with the *o*-quinone and semiquinone ligands in the accessibility of the fully reduced amidophenolate or catecholate analogue. The reduction potential for the PhenoxSQ anion is considerably more negative than the Cat/SQ couple of the quinone ligands. Reduction of Ru(PPh$_3$)Cl(PhenoxSQ)$_2$ occurs at the metal to give a nucleophilic Ru(II) complex, while reduction of a corresponding Ru^{III}(SQ)$_2$ species occurs at the quinone ligands giving a much less reactive product. Oxidation reactions that utilize molecular oxygen are of commercial interest,[17] and they are pertinent to the stereoselective substrate oxidation reactions of enzymes.[18] The striking and surprising oxidation reaction leading to formation of the OxPhenox ligand may parallel the oxidation of coordinated catechol ligands. Generally, oxidative cleavage of the ring occurs at the C–C bond internal to the chelate ring in a manner that is typical of the intradiol dioxygenase enzymes. The reaction leading to the OxPhenox ligand proceeds by cleavage of the ring bond exterior to the chelate ring to give a product that might arise from a reaction that parallels the extradiol dioxygenase enzymes. Selectivity in this reaction appears to result from the effects of intramolecular hydrogen bonding with steric direction provided by the triphenylphosphine ligand and the Phenox *tert*-butyl groups. This combination of properties contributes to the formation of a single diasteromeric product with three chiral centers.

Acknowledgment. We gratefully acknowledge the help of Dr. Steven Boone with the crystallographic investigations. This research was supported by the National Science Foundation through Grants CHE-88-09923 and CHE-90-23636; ruthenium trichloride was provided by Johnson Matthey, Inc., through their Metal Loan Program.

Supplementary Material Available: Tables giving crystal data and details of the structure determination, anisotropic thermal parameters, hydrogen atom locations, and bond lengths and angles for PhenoxBQ, Ru(PPh$_3$)$_2$Cl$_2$(PhenoxSQ), and Ru(PPh$_3$)Cl(Phenox)$_2$ (47 pages); listings of observed and calculated structure factors (49 pages). Ordering information is given on any current masthead page.

---

(17) Riley, D. P.; Fields, D. L.; Rivers, W. *J. Am. Chem. Soc.* **1991**, *113*, 3371.

(18) Smith, J. R. L.; Mortimer, D. N. *J. Chem. Soc., Chem. Commun.* **1985**, 64.

Contribution from the Departments of Chemistry, Southwest Texas State University, San Marcos, Texas 78666,
Howard University, Washington, D.C., and Keene State College, Keene, New Hampshire 03431

Synthesis, Structure, and Spectroscopic Properties of Vanadium(III) and -(IV) Complexes Containing Hydridotris(pyrazolyl)borate Ligands. 3

Madan Mohan,[†] Stephen M. Holmes,[†] Ray J. Butcher,[‡] Jerry P. Jasinski,[§] and Carl J. Carrano*[,†]

Received September 26, 1991

A series of vanadium(III) and -(IV) complexes of the type [L$_2$V]BPh$_4$, [LVCl$_2$DMF], [LVOClDMF], and [LVO(acac)] where L is either the anion of hydridotris(pyrazolyl)borate, HB(pz)$_3$, or hydridotris(3,5-dimethylpyrazolyl)borate, HB(Me$_2$pz)$_3$, have been synthesized and characterized by elemental analysis, molar conductance, electrochemistry, magnetic, UV–vis, IR, and ESR techniques. In all cases, the metal ion is in a distorted octahedral environment, facially coordinated to a tridentate hydridotris(pyrazolyl)borate ligand of varying steric bulk. The structures of the complexes of the type [L$_2$V]BPh$_4$ have been determined by single-crystal X-ray diffraction. Crystal data for [[HB(pz)$_3$]$_2$V]BPh$_4$ are as follows: space group $P\bar{1}$ with $a = 12.796$ (1) Å, $b = 15.305$ (2) Å, $c = 11.285$ (1) Å, $\alpha = 94.38$ (1)°, $\beta = 104.248$ (9)°, $\gamma = 108.64$ (1)°, $V = 2000.7$ (5) Å^3, and $Z = 2$. In general, comparison of the structural and physicochemical properties among the series reveals the expected effects of the electron-releasing methyl groups but few if any differences between analogous complexes that can be attributed to steric bulk. However, electrochemistry does demonstrate significant differences between the unsubstituted and 3,5-dimethyl-substituted derivatives not evident from structural parameters which indicate a reduced access to the metal in the latter. The significance of these data to our understanding of vanadium centers in biological systems is discussed.

In a series of previous publications,[1-3] we and others have examined some of the chemistry of vanadium(III), -(IV), and -(V) with the hydridotris(3,5-dimethylpyrazolyl)borate ligand as a model for vanadium–histidine interactions that could be present in proteins such as the haloperoxidases from marine algae and terrestrial lichens.[4-7] Most of these complexes contain the hydridotris(3,5-dimethylpyrazolyl)borate group coordinated to the vanadium in a tridentate fashion leaving open another three coordination sites for ancillary ligands to complete a distorted octahedral environment around the metal ion. Since one of the unique ligating effects of a protein involves its ability to restrict access to a metal center, we were curious how such steric effects might be reflected in the structural and/or physicochemical properties of model complexes. Accordingly, we have synthesized and examined a series of analogous complexes using both the unsubstituted and the 3,5-dimethyl-substituted pyrazolylborate ligands. These ligands have respective "wedge angles" of 120° and 91° which reflect in a qualitative way the ease of access to the metal.[8] In this paper, we report that while structural differences between the substituted and unsubstituted complexes are insignificant, electrochemistry clearly reveals an increased accessibility to the metal center in the latter. It is anticipated that these results may aid in our understanding of the nature of va-

---

[†] Southwest Texas State University.

[‡] Howard University.

[§] Keene State College.

(1) Kime-Hunt, E.; Spartalian, K.; DeRusha, M.; Nunn, C. M.; Carrano, C. J. *Inorg. Chem.* **1989**, *28*, 4392.

(2) Holmes, S. M.; Carrano, C. J. *Inorg. Chem.* **1991**, *30*, 1231.

(3) Collison, D.; Mabbs, F. E.; Passand, M. A.; Rigby, K.; Cleland, W. E. *Polyhedron* **1989**, *8*, 1827.

(4) Vilter, H. *Phytochemistry* **1984**, *23*, 1387.

(5) Plat, H.; Krenn, B. E.; Wever, R. *Biochem. J.* **1987**, *248*, 277.

(6) van Kooyk, Y.; de Boer, E.; Tromp, M. G. M.; Plat, H.; Wever, R. *Biochim. Biophys. Acta* **1986**, *869*, 48.

(7) Butler, A.; Carrano, C. J. *Coord. Chem. Rev.* **1991**, *109*, 61.

(8) Calabrese, J. C.; Domaille, P. J.; Trofimenko, S.; Long, G. J. *Inorg. Chem.* **1991**, *30*, 2795.

0020-1669/92/1331-2029$03.00/0

nadium-binding sites in proteins and other biomolecules.

Experimental Section

Materials. All synthetic reactions were carried out under an atmosphere of pure dry argon or nitrogen by utilizing standard Schlenk techniques. Subsequent work-up was carried out in air unless otherwise noted. Solvents were dried and distilled under a blanket of inert gas. DMF and acetonitrile were Burdick and Jackson "distilled in glass" grade and used as received. They were stored under an argon atmosphere after opening. Potassium hydridotris(3,5-dimethylpyrazolyl)borate and unsubstituted tris(pyrazolyl)borate were synthesized and purified according to the reported methods.[9,10] Vanadium salts were reagent grade and used as received.

Synthesis. [[HB(3,5-Me$_2$pz)$_3$]$_2$V]BPh$_4$, I. To 10 mL of dry acetonitrile (ACN) was added vanadium trichloride (1.2 g, 7.64 mmol), and the mixture was heated under reflux until a green solution of [VCl$_3$(ACN)$_3$] was formed. To this solution was added potassium hydridotris(3,5-dimethylpyrazolyl)borate (5.0 g, 14.85 mmol), and the mixture was heated under reflux for an additional 3 h. The green solution turned dark yellow-brown during this time period. The yellow solution was filtered through Celite, and an excess of sodium tetraphenylborate in methanol was added which precipitated a bright yellow solid. The solid was filtered off, redissolved in chloroform, and overlayered with methanol. The solution was allowed to stand at room temperature for several hours and produced a crop of deep yellow-brown crystals. The crystals were collected by filtration and dried in air. Yield: 4.45 g (62.0%). Anal. Calcd for $C_{54}H_{64}N_{12}B_3V$: C, 67.21; H, 6.63; N, 17.42; V, 5.29. Found: C, 66.99; H, 6.71; N, 17.39; V, 6.0. mp 320–321 °C.

The unsubstituted pyrazolylborate analogue, [[HB(pz)$_3$]$_2$V]BPh$_4$, II, was synthesized and crystallized in a similar fashion. In this case deep red crystals were obtained, suitable for X-ray diffraction. Yield: 3.71 g (61.2%). mp 250–252 °C.

[[HB(3,5-Me$_2$Pz)$_3$]VCl$_2$DMF], III. This compound has been reported previously by us but the following represents an improved synthesis.[1] To a solution of vanadium trichloride (5.0 g; 31.7 mmol) in 150 mL of dry DMF was added, with constant stirring, an equimolar quantity of K-[HB(3,5-Me$_2$pz)$_3$] (10.67 g; 31.7 mmol). A deep purple solution resulted which was stirred overnight. The solution was then exposed to the air for 6 h during which time it turned a deep green. The solution was filtered through Celite to remove KCl, and the solvent DMF was removed under vacuum. The resulting green solid was dissolved in dry CH$_2$Cl$_2$ and filtered once again through Celite to remove the last traces of KCl. The solution was concentrated and overlayered with Et$_2$O to afford a green crystalline solid. The solid was collected by filtration, washed with Et$_2$O and dried under vacuum. Yield: 9.10 g (58.3%).

[[HB(pz)$_3$]VCl$_2$DMF]·$^1/_4$CH$_2$Cl$_2$, IV. To a solution of vanadium trichloride (5.0 g; 31.7 mmol) in 100 mL of dry DMF was added, with constant stirring, an equimolar quantity of [HB(pz)$_3$] (8.0 g; 31.7 mmol), and the resulting deep purple solution was stirred overnight. The solution was then exposed to air and stirred for an additional 12 h. During this period of time, the deep purple solution turned dark green, and a large quantity of green solid precipitated. The solid was filtered, dried, and redissolved in dry CH$_2$Cl$_2$. The resulting solution was filtered through Celite to remove KCl and concentrated to afford the solid product. The solid was collected, washed with CH$_2$Cl$_2$ and Et$_2$O, and air dried. Yield: 8.0 g (58.7%). Anal. Calcd. for $C_{12}H_{17}N_7BOVCl_2\cdot{}^1/_4CH_2Cl_2$: C, 34.27; H, 4.07; N, 22.84; V, 11.88. Found: C, 34.54; H, 4.04; N, 23.03 V; 11.33. mp 209–211 °C.

[[HB(pz)$_3$]VO(acac)], V. To the solution of K[(HB(pz)$_3$] (5.04 g; 20 mmol) in 30 mL of dry methanol was added a solution of VO(acac)$_2$ (5.30 g; 20 mmol) in 25 mL of dry MeOH, and the resulting blue green solution mixture was heated under reflux with constant stirring. The mixture gradually became violet, and a violet-colored solid precipitated. The mixture was heated for an additional 2 h to ensure complete formation of the complex. The solid was filtered, washed with MeOH and Et$_2$O, and air dried. Recrystallization was from ACN. Yield: 4.19 g (55.4%). Anal. Calcd for $C_{14}H_{17}N_6BVO_3$: C, 44.32; H, 4.48; N, 22.16. Found: C, 44.68; H, 4.43; N, 22.39. mp 273 °C.

[[HB(pz)$_3$]VO(Cl)DMF], VII. A procedure similar to that used to prepare IV was also used to isolate the V(IV) complex except that the deep purple solution was exposed to the air for an additional 48 h with constant stirring. Alternatively, this complex could be prepared by aerial oxidation (48 h) of IV in methylene chloride. The green solution was filtered through Celite, concentrated, and layered with Et$_2$O to afford a blue-green solid. The solid was filtered, washed with Et$_2$O, and air dried. Crystallization from methylene chloride/hexane yielded light blue needles. Yield: 7.5 g (61.0%).

Table I. Crystallographic Data for II

$C_{42}H_{40}N_{12}B_3V$	$V = 2000.7$ (5) Å^3
fw = 796.23	$Z = 2$
$a = 12.796$ (1) Å	$P\bar{1}$ no. 2
$b = 15.305$ (2) Å	$T = 23$ °C
$c = 11.285$ (1) Å	$\lambda = 0.71069$ Å
$\alpha = 94.38$ (1)°	$\rho_{calcd} = 1.318$ g/cm^3
$\beta = 104.248$ (9)°	$\mu = 2.84$ cm^{-1}
$\gamma = 108.64$ (1)°	$R(F_o) = 0.041$
	$R_w(F_o) = 0.048$

The compounds [[HB(3,5-Me$_2$pz)$_3$]VO(Cl)DMF], VIII, and [[HB-(3,5-Me$_2$pz)$_3$]VO(acac)], VI, were synthesized according to the reported procedures.[1] Attempts to prepare vanadium tris(pyrazolyl)borate complexes of ligands more sterically demanding than the 3,5-dimethyl or unsubstituted analogues have met with continued failure. Reaction of vanadium(III) or -(IV) salts with the 3-*tert*-butyl-, phenyl-, or isopropyl-substituted tris(pyrazolyl)borates invariably resulted in B–N bond cleavage, producing mono- or dinuclear *pyrazole* complexes (the isolation and characterization of these species will be the subject of a separate report).

Collection and Reduction of X-ray Data. A data crystal of II was obtained as described above, epoxyed to a glass fiber, and transferred to a Rigaku AFC6S diffractometer employing graphite monochromated Mo Kα radiation. Data collection procedures have been previously described.[11] Cell constants and an orientation matrix were obtained from a least-squares refinement of 25 carefully centered reflections in the range of $40 < 2\theta < 44°$. Crystal data and collection parameters are summarized in Table I.

Solution and Refinement of Structure. Data were reduced and the models refined using the TEXSAN program package. On the basis of packing considerations, a statistical analysis of the intensity distribution, and the successful solution and refinement of the structure, the space group was determined to be $P\bar{1}$. The structure was solved using the direct methods program, SHELXS of George Sheldrick and refined using full matrix least-squares refinement. Hydrogen atoms were initially generated at idealized positions and allowed to refine isotropically. Fractional atomic coordinates for II are given in Table II. Selected bond distances and angles are displayed in Table III. Detailed data for II are found in the Supplementary Material.

Physical Measurements. Electrochemical measurements employed either a BAS CV-27 electrochemical analyzer (CV measurements) or a PWR-3 power potentiostat (bulk electrolysis). Cyclic voltammetry, using Pt bead electrodes, was performed as previous described.[12] Tetrabutylammonium hexafluorophosphate was used as a supporting electrolyte. Potentials are versus the SCE and are referenced to the ferrocene/ferrocenium couple employed as an external standard. UV–vis spectra were recorded on a Perkin-Elmer 553 spectrophotometer, while infrared spectra employed a PE model 1600 FT-IR with samples prepared as KBr pellets. ESR data were recorded on a Brucker ER200 E-SRC spectrometer equipped with a liquid nitrogen Dewar and variable temperature apparatus. Initial estimates of the parameters for these nearly axial systems were obtained by inspection; final fitting of the rhombic spectra utilized either the program EPRPOW as modified by K. Spartalian, Department of Physics, University of Vermont, or ESR (Calleo Scientific Software). Spectra were recorded at ca. 110 K. Solid-state magnetic moments were calculated from data obtained on a Johnson-Matthey MSB-1 magnetic susceptibility balance.

Results and Discussion

Description of Structure. [[HB(pz)$_3$]$_2$V]BPh$_4$. Figure 1 shows the atom labeling scheme for the cationic portion of the title compound. The tetraphenylborate anion is not shown. There are two independent molecules of the vanadium complex in the unit cell; however, there are no significant differences between them. Selected bond lengths and angles are summarized in Table III. The two six-coordinate vanadium atoms lie on crystallographically imposed inversion centers and are encapsulated by the tridentate pyrazolylborates. The V–N bonds range from 2.055 to 2.095 Å, averaging 2.079 Å in molecule A and 2.068 Å in molecule B. The N–V–N bond angles range from 84.96° to 94.04°. The corresponding values for the methoxide salt[13] of the 3,5-dimethyl-

---

(9) Trofimenko, S. *J. Am. Chem. Soc.* **1967**, *22*, 6288.

(10) Trofimenko, S. *Inorg. Syn.* **1970**, *12*, 99.

(11) Jasinski, J. *J. Org. Chem.* **1991**, *56*, 710.

(12) Bonadies, J. A.; Carrano, C. J. *J. Am. Chem. Soc.* **1986**, *108*, 4088.

(13) The methoxide salt of the 3,5-dimethyl-substituted complex was isolated as a decomposition product from the treatment of VIII or VI with *tert*-butylhydroperoxide in methylene chloride.

Table II. Positional Parameters and *B* (eq) for II

atom	*x*	*y*	*z*	*B* (eq)
V (1A)	1/2	1/2	1.0000	2.53 (2)
V (1B)	1.000	0	0	2.73 (2)
N (1A)	0.3811 (2)	0.4600 (1)	0.8234 (2)	2.98 (7)
N (1B)	0.6271 (2)	0.5245 (1)	0.9096 (2)	2.99 (7)
N (1C)	0.4990 (2)	0.3644 (1)	0.9841 (2)	2.82 (7)
N (1D)	1.1471 (2)	−0.0286 (1)	0.0722 (2)	3.24 (7)
N (1E)	1.0480 (2)	0.0950 (1)	0.1622 (2)	3.30 (7)
N (1F)	0.9197 (2)	−0.0986 (1)	0.0954 (2)	3.16 (7)
N (2A)	0.3970 (2)	0.4039 (1)	0.7342 (2)	2.84 (7)
N (2B)	0.6107 (2)	0.4635 (1)	0.8059 (2)	3.06 (7)
N (2C)	0.5005 (2)	0.3212 (1)	0.8739 (2)	2.90 (7)
N (2D)	1.1751 (2)	−0.0398 (1)	0.1942 (2)	3.32 (7)
N (2E)	1.0900 (2)	0.0697 (1)	0.2731 (2)	3.20 (7)
N (2F)	0.9765 (2)	−0.0993 (1)	0.2148 (2)	3.24 (7)
C (1J)	0.8028 (2)	0.2955 (2)	0.3389 (2)	2.69 (8)
C (1H)	0.7913 (2)	0.2686 (2)	0.5732 (2)	2.54 (8)
C (1I)	0.6046 (2)	0.2525 (2)	0.3877 (2)	2.76 (8)
C (1G)	0.7140 (2)	0.1238 (2)	0.3978 (2)	2.71 (8)
C (2H)	0.9083 (2)	0.2886 (2)	0.6248 (2)	3.38 (9)
C (2I)	0.6037 (2)	0.3427 (2)	0.4183 (2)	3.32 (9)
C (2J)	0.7706 (2)	0.2645 (2)	0.2110 (2)	3.8 (1)
C (2G)	0.7863 (2)	0.0921 (2)	0.3464 (3)	3.7 (1)
C (3J)	0.8237 (3)	0.3137 (2)	0.1319 (3)	4.5 (1)
C (3I)	0.5049 (2)	0.3643 (2)	0.3924 (3)	4.3 (1)
C (3G)	0.7807 (3)	0.0006 (2)	0.3320 (3)	4.5 (1)
C (3H)	0.9632 (2)	0.3162 (2)	0.7509 (3)	4.0 (1)
C (3A)	0.3106 (2)	0.3860 (2)	0.6306 (3)	3.7 (1)
C (3B)	0.7037 (2)	0.4924 (2)	0.7653 (3)	3.9 (1)
C (3C)	0.4991 (2)	0.2349 (2)	0.8857 (3)	3.6 (1)
C (3D)	1.2711 (3)	−0.0599 (2)	0.2195 (3)	4.7 (1)
C (3E)	1.1085 (2)	0.1389 (2)	0.3649 (3)	4.1 (1)
C (3F)	0.9068 (2)	−0.1646 (2)	0.2599 (3)	3.6 (1)
C (4H)	0.9002 (3)	0.3232 (2)	0.8312 (3)	4.4 (1)
C (4G)	0.7007 (3)	−0.0664 (2)	0.3694 (3)	4.1 (1)
C (4I)	0.4001 (2)	0.2963 (2)	0.3356 (3)	4.7 (1)
C (4J)	0.9129 (2)	0.3971 (2)	0.1762 (3)	4.3 (1)
C (4A)	0.2363 (2)	0.4290 (2)	0.6490 (3)	4.2 (1)
C (4B)	0.7821 (2)	0.5718 (2)	0.8413 (3)	4.3 (1)
C (4C)	0.4961 (2)	0.2195 (2)	1.0024 (3)	4.0 (1)
C (4D)	1.3081 (3)	−0.0625 (2)	0.1164 (3)	5.2 (1)
C (4E)	1.0803 (3)	0.2097 (2)	0.3158 (3)	4.5 (1)
C (4F)	0.8041 (2)	−0.2075 (2)	0.1712 (3)	3.9 (1)
C (5I)	0.3976 (2)	0.2078 (2)	0.3027 (3)	4.8 (1)
C (5J)	0.9475 (3)	0.4306 (2)	0.3013 (3)	4.2 (1)
C (5H)	0.7838 (3)	0.3014 (2)	0.7848 (3)	4.6 (1)
C (5G)	0.6290 (2)	−0.0387 (2)	0.4236 (3)	4.0 (1)
C (5A)	0.2839 (2)	0.4749 (2)	0.7702 (3)	3.7 (1)
C (5B)	0.7309 (2)	0.5891 (2)	0.9294 (3)	3.7 (1)
C (5C)	0.4973 (2)	0.3026 (2)	1.0619 (3)	3.6 (1)
C (5D)	1.2287 (2)	−0.0426 (2)	0.0270 (3)	4.1 (1)
C (5E)	1.0419 (2)	0.1800 (2)	0.1891 (3)	3.9 (1)
C (5F)	0.8158 (2)	−0.1638 (2)	0.0708 (3)	3.5 (1)
C (6H)	0.7307 (2)	0.2752 (2)	0.6587 (2)	3.5 (1)
C (6J)	0.8926 (2)	0.3805 (2)	0.3801 (2)	3.53 (9)
C (6G)	0.6363 (2)	0.0539 (2)	0.4366 (2)	3.46 (9)
C (6I)	0.4969 (2)	0.1860 (2)	0.3267 (3)	3.6 (1)
B (1A)	0.5031 (3)	0.3740 (2)	0.7627 (3)	3.0 (1)
B (1B)	1.0991 (3)	−0.0285 (2)	0.2775 (3)	3.5 (1)
B (1C)	0.7275 (2)	0.2340 (2)	0.4235 (3)	2.61 (9)
H (2H)	0.951 (2)	0.279 (2)	0.573 (2)	3.9 (6)
H (2J)	0.711 (2)	0.204 (2)	0.177 (2)	3.8 (6)
H (2I)	0.678 (2)	0.393 (1)	0.458 (2)	2.1 (5)
H (2G)	0.841 (2)	0.134 (2)	0.325 (2)	4.5 (7)
H (3J)	0.798 (2)	0.290 (2)	0.046 (3)	5.5 (7)
H (3G)	0.839 (2)	−0.014 (2)	0.304 (2)	5.3 (7)
H (3I)	0.510 (2)	0.426 (2)	0.418 (2)	4.3 (6)
H (3H)	1.046 (2)	0.332 (2)	0.777 (2)	4.0 (6)
H (3A)	0.309 (2)	0.351 (2)	0.564 (2)	3.5 (6)
H (3B)	0.709 (2)	0.456 (2)	0.702 (2)	3.2 (6)
H (3C)	0.500 (2)	0.200 (2)	0.819 (2)	3.8 (6)
H (3D)	1.298 (2)	−0.071 (2)	0.293 (3)	5.8 (8)
H (3E)	1.132 (3)	0.127 (2)	0.441 (3)	7 (1)
H (3F)	0.939 (2)	−0.171 (2)	0.342 (2)	4.4 (7)
H (4H)	0.936 (2)	0.342 (2)	0.913 (2)	4.8 (7)
H (4I)	0.331 (2)	0.312 (2)	0.319 (2)	3.7 (6)
H (4G)	0.695 (2)	−0.130 (2)	0.358 (2)	3.8 (6)
H (4J)	0.953 (2)	0.436 (2)	0.123 (3)	6.1 (8)
H (4A)	0.170 (2)	0.431 (2)	0.585 (2)	5.1 (7)
H (4B)	0.856 (2)	0.608 (2)	0.836 (2)	4.3 (6)
H (4C)	0.497 (2)	0.166 (2)	1.041 (2)	4.3 (6)
H (4D)	1.370 (2)	−0.077 (2)	0.106 (3)	6.2 (8)
H (4E)	1.087 (2)	0.268 (2)	0.353 (2)	4.7 (7)
H (4F)	0.739 (2)	−0.254 (2)	0.173 (2)	3.4 (6)
H (5I)	0.332 (2)	0.165 (2)	0.263 (2)	4.7 (7)
H (5H)	0.738 (2)	0.307 (2)	0.843 (3)	5.9 (8)
H (5J)	1.006 (2)	0.488 (2)	0.331 (2)	5.3 (7)
H (5G)	0.575 (2)	−0.085 (2)	0.452 (2)	5.1 (7)
H (5A)	0.263 (2)	0.511 (2)	0.817 (2)	3.5 (6)
H (5B)	0.762 (2)	0.637 (1)	0.992 (2)	2.6 (5)
H (5C)	0.499 (2)	0.321 (2)	1.141 (2)	3.8 (6)
H (5D)	1.228 (2)	−0.038 (2)	−0.053 (2)	3.7 (6)
H (5E)	1.015 (2)	0.209 (2)	0.121 (2)	4.8 (7)
H (5F)	0.764 (2)	−0.177 (1)	−0.002 (2)	2.7 (5)
H (6H)	0.647 (2)	0.262 (2)	0.625 (2)	4.1 (6)
H (6G)	0.584 (2)	0.068 (2)	0.471 (2)	3.1 (6)
H (6J)	0.920 (2)	0.411 (2)	0.462 (2)	3.5 (6)
H (6I)	0.495 (2)	0.126 (2)	0.302 (2)	3.9 (6)

Table III. Selected Bond Lengths and Angles Involving the Coordination Sphere of II[a]

atom	atom	distance	atom	atom	atom	angle
V1A	N1A	2.095 (2)	N1A	V1A	N1A	180.00
V1A	N1B	2.076 (2)	N1A	V1A	N1B	86.66 (8)
V1A	N1C	2.065 (2)	N1A	V1A	N1B	93.34 (8)
V1B	N1D	2.055 (2)	N1A	V1A	N1C	86.87 (8)
V1B	N1E	2.076 (2)	N1A	V1A	N1C	93.13 (8)
V1B	N1F	2.073 (2)	N1B	V1B	N1B	180.00
			N1B	V1A	N1C	84.96 (8)
			N1B	V1A	N1C	95.04 (8)
			N1D	V1B	N1D	180.00
			N1D	V1B	N1E	87.02 (8)
			N1D	V1B	N1E	92.98 (8)
			N1D	V1B	N1F	87.25 (8)
			N1D	V1B	N1F	92.75 (8)
			N1E	V1B	N1E	180.00
			N1E	V1B	N1F	85.85 (8)
			N1E	V1B	N1F	94.15 (8)

[a] Bond lengths are in angstroms, and angles are in degrees. Estimated standard deviations in the least significant figure are given in parentheses.

substituted complex, also solved by us (data not shown), are virtually identical with an average V–N bond of 2.083 Å and an average N–V–N angle of 88.4°.

We and others have previously reported on the 3,5-dimethyl-substituted analogue [[HB(3,5-$Me_2pz)_3$]VO(acac)], the structure of which has been determined by Mabbs et al.[14] We have completed a structure of the unsubstituted analogue (data not shown) to see if there were any discernable effects caused by the decreased cone angle for the HB$(pz)_3$ moiety as compared to HB$(Me_2pz)_3$.[15] None were evident, and the structure was virtually identical to that previously reported; hence data have not been tabulated. Indeed a comparison among the structures of analogous complexes of the unsubstituted and hydridotris(3,5-dimethylpyrazolyl)borates reveal no significant structural differences attributable to steric effects. Nevertheless, significant differences in stabilities are noted (vide infra).

Physical and Spectroscopic Properties. Most of the complexes reported here possess sharp melting points and are quite stable at room temperature in the solid state and do not show any sign of decomposition even after prolonged storage. However, complex IV is oxidized to VII over the course of time. The complexes are

---

(14) Beddoes, R. L.; Collison, D.; Mabbs, F. E.; Passand, M. A. *Polyhedron* **1990**, *4*, 2483.

(15) Crystal data for HB$(pz)_3$VO(acac): Space group $P_{2_1/n}$ with a = 7.649 (3) Å, b = 7.024 (4) Å, c = 13.380 (3) Å, β = 92.11^{6}, V = 1741 (1), R = 5.2%, and R_w = 5.05%.

Table IV. Electronic Spectral Data for V(III) and V(IV) Complexes (in CH_2Cl_2)

complexes	bands, cm^{-1}	ϵ, $dm^3\ mol^{-1}\ cm^{-1}$	assignments		*Dq*, cm^{-1}
$[[HB(pz)_3]VO(Cl)DMF]$	14 080	54.70	$^2B_2$	$\rightarrow {}^2E$	1750
	17 498	42.20		$\rightarrow {}^2B_1$	
	22 138 sh	31.60		$\rightarrow {}^2A_1$	
$[[HB(pz)_3]VO(acac)]$	13 330	35.65	$^2B_2$	$\rightarrow {}^2E$	1850
	18 500	16.62		$\rightarrow {}^2B_1$	
	25 381 sh	43.14		$\rightarrow {}^2A_1$	
$[[HB(3,5\text{-}Me_2pz)_3]VO(Cl)DMF]$	13 122	47.96	$^2B_2$	$\rightarrow {}^2E$	1697
	16 966	26.61		$\rightarrow {}^2B_1$	
	25 640 sh	46.97		$\rightarrow {}^2A_1$	
$[[HB(3,5\text{-}Me_2pz)_3]VO(acac)]$	12 903	56.00	$^2B_2$	$\rightarrow {}^2E$	1786
	17 857	13.20		$\rightarrow {}^2B_1$	
	24 875	51.44		$\rightarrow {}^2A_1$	
$[[HB(pz)_3]VCl_2DMF]$	16 393	38.5	$^3T_{1g}$	$\rightarrow {}^3T_{2g}$	1754
	23 256	76.11		$\rightarrow {}^3T_{1g}$	
	33 940[a]			$\rightarrow {}^3A_{2g}$	
$[[HB(3,5\text{-}Me_2pz)_3]VCl_2DMF]$	15 888	20.23	$^3T_{1g}$	$\rightarrow {}^3T_{2g}$	1719
	24 284	236.22		$\rightarrow {}^3T_{1g}$	
	33 080[a]			$\rightarrow {}^3A_{2g}$	

[a] Calculated.

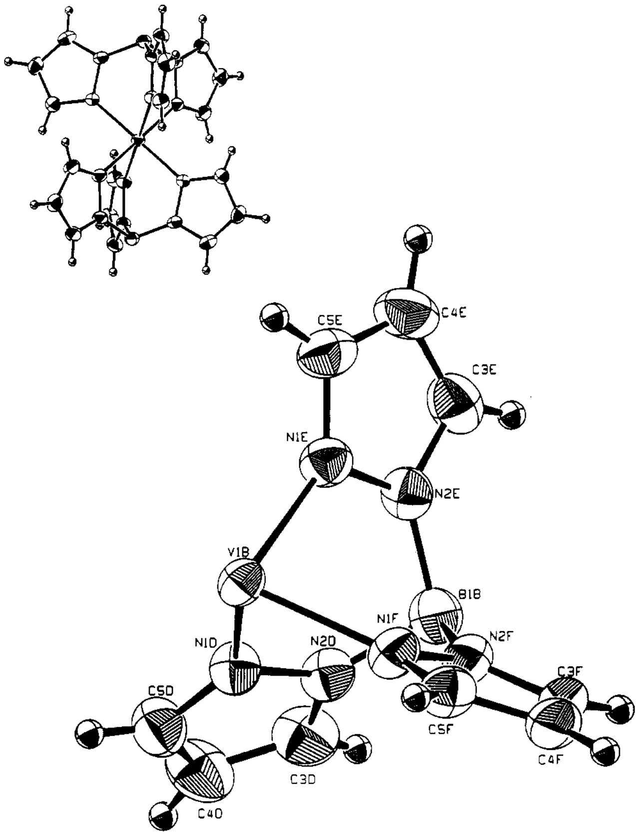

Figure 1. ORTEP plot of the cationic portion of $[[HB(pz)_3]_2V]BPh_4$ showing the atom labeling scheme for one of two independent molecules in the unit cell. The inset shows the coordination geometry around the vanadium.

soluble in a number of solvents of moderate-to-good polarity such as dimethylformamide, dimethyl sulfoxide, dichloromethane, ethanol, and methanol. The molar conductances of ca. 10^{-3} M solutions of complexes III–VIII in dimethylformamide at room temperature lie in the range 20–35 $\Omega^{-1}\ cm^2\ mol^{-1}$, while for I and II they are in the range 75–95 $\Omega^{-1}\ cm^2\ mol^{-1}$, indicating their nonelectrolytic and uni-univalent behavior in solution, respectively.[16] The room temperature magnetic moments of 1.78–1.80 μ_B observed for complexes V–VIII are characteristic of magnetically dilute, distorted octahedral V(IV) complexes (the spin-only value for d^1 is 1.73 μ_B), while those of ca. 2.8 μ_B for for complexes I–IV indicate mononuclear, octahedral vanadium(III) (the spin-only value for such d^2 species is 2.83 μ_B).

The solid-state infrared spectra of all the complexes exhibit a B–H stretching absorption in the range 2500–2550 cm^{-1}. The tris coordination of the pyrazolylborate group is indicated by the appearance of an aromatic ν (C–N) stretch at ca. 1500 cm^{-1} in the unsubstituted pyrazolylborate and near 1540 cm^{-1} for the 3,5-dimethyl derivatives. A very strong absorption at ca. 1650 cm^{-1} indicates the coordination of solvent DMF in complexes III, IV, VII, and VIII. The complexes V–VIII also exhibit a strong band in the range 970–990 cm^{-1} which is assigned to the V=O stretch.

The visible spectra of complexes V–VIII in dichloromethane show the characteristic series of absorption bands common to vanadyl systems, designated as bands I, II, and III.[17-20] In terms of the Ballhausen and Gray model,[24] accordingly, the first absorption band occurring in the 13 000–14 000-cm^{-1} region can be assigned to the electronic transition $^2B_2 \rightarrow {}^2E$ (or $b_2 \rightarrow e_\pi^*$), the second in the 17 500–18 500-cm^{-1} region to the $^2B_2 \rightarrow {}^2B_1$ (or $b_2 \rightarrow b_1^*$) transition, and the third in the 22 000–25 000-cm^{-1} region to the $^2B_2 \rightarrow {}^2A_1$ (or $b_2 \rightarrow a_1^*$). The spectral data and calculated *Dq* values have been detailed in Table IV.[25,26]

The V(III) complexes III and VI in dichloromethane show two absorption bands, one between 15 000 and 16 000 cm^{-1} and another in the 23 000–24 500-cm^{-1} region, which have been assigned in a pseudooctahedral environment to the $^3T_{1g} \rightarrow {}^3T_{2g}$ and $^3T_{1g} \rightarrow {}^3T_{1g}(P)$ transitions, respectively. The expected $^3T_{1g} \rightarrow {}^3A_{2g}$ is a two-electron transition and should thus be very weak and occurs at a frequency where it is expected to be obscured by charge-transfer or intraligand transitions. It is not observed in the present complexes. In complexes I and II, no d–d bands are observed at all, and only charge-transfer bands are visible. Detailed spectral data are also given in Table IV.

The complexes V–VIII exhibit similar eight-line isotropic ESR

---

(16) Geary, W. J. *Coord. Chem. Rev.* **1971**, *7*, 81.

(17) Ballhausen, C. J.; Gray, H. B. *Inorg. Chem.* **1962**, *1*, 111.

(18) Kuska, H. A.; Yang, Y. P. *Inorg. Chem.* **1974**, *13*, 1090.

(19) Donini, J. C.; Hollebone, B. R.; London, G.; Lever, A. B. P.; Hampel, J. C. *Inorg. Chem.* **1975**, *14*, 455.

(20) Lever, A. B. P. *Inorganic Electronic Spectroscopy*; Elsevier: New York, 1984.

(21) Li, X.; Lah, M. S.; Pecoraro, V. L. *Inorg. Chem.* **1988**, *27*, 4657.

(22) Arber, J. M.; deBoer, E.; Garner, E.; Hasnain, C. D.; Wever, R. *Biochemistry* **1989**, *28*, 7968.

(23) Tromp, M. G. M.; Olafsson, G.; Krenn, B. E.; Wever, R. *Biochim. Biophys. Acta* **1990**, *1040*, 192.

(24) Selbin, J. *Chem. Rev.* **1965**, *65*, 153.

(25) Selbin, J. *Coord. Chem. Rev.* **1966**, *1*, 293.

(26) Cooper, S. R.; Koh, Y. B.; Raymond, K. N. *J. Am. Chem. Soc.* **1982**, *104*, 5092.

Table V. ESR Parameters for V(IV) Complexes

	[[HB(pz)$_3$]-VO(Cl)DMF]	[[Hb(pz)$_3$]-VO(acac)]	[[HB(3,5-Me$_2$pz)$_3$]-VO(Cl)DMF]	[[HB(3,5-Me$_2$pz)$_3$]-VO(acac)]
g_1	1.9459	1.9470	1.9500	1.9501
g_2	1.9862	1.9877	1.9820	1.9832
g_3	1.9851	1.9820	1.9820	1.9804
$A_1/10^{-4}$ cm^{-1}	161.9	162.2	164.1	164.3
$A_2/10^{-4}$ cm^{-1}	57.3	57.7	56.8	58.6
$A_3/10^{-4}$ cm^{-1}	56.2	55.8	55.6	55.9
$\langle g \rangle$	1.9724	1.9722	1.9713	1.9712
$\langle A \rangle$	99.93	100.00	100.26	101.13

Table VI. Electrochemical Data

	complex	$E°$ (V)	solvent
(I)	[[HB(pz)$_3$]$_2$V]BPh$_4$	−0.42	ACN
		−0.30	CH$_2$Cl$_2$
		−0.29	DMF
(II)	[[HB(Me$_2$pz)$_3$]$_2$V]BPh$_4$	−0.69	ACN
		−0.68	CH$_2$Cl$_2$
		−0.51	DMF
(III)	[[HB(Me$_2$pz)$_3$]VCl$_2$DMF]	1.13	
		1.28	ACN
		1.22	CH$_2$Cl$_2$
(IV)	[[HB(pz)$_3$]VCl$_2$DMF]	1.27	
		1.47	ACN
		1.28	CH$_2$Cl$_2$
(V)	[[HB(pz)$_3$]VO(acac)]	1.23	ACN
		1.21	CH$_2$Cl$_2$
		1.32 (irr)	DMF
(VI)	[[HB(Me$_2$pz)$_3$]VO(acac)]	1.11	ACN
		1.07	CH$_2$Cl$_2$
		1.19	DMF
(VII)	[[HB(pz)$_3$]VO(Cl)DMF]	1.33	ACN
		1.33	CH$_2$Cl$_2$
(VIII)	[[HB(Me$_2$pz)$_3$]VO(Cl)DMF]	1.03	ACN
		1.21	CH$_2$Cl$_2$

spectra in dichloromethane, indicating the presence of a d^1 (V(IV) (nearly 100% $I = {}^7/_2$) nucleus. The frozen solution spectra are generally axial with a slight rhombicity and are typical of vanadyl complexes. The values of the principal components of $\langle g \rangle$ tensor and the hyperfine interaction tensor $\langle A \rangle$ are given in Table V.

Electrochemistry. The electrochemical properties of vanadium(IV) complexes V–VIII are similar in that they display an almost reversible redox process corresponding to oxidation of the metal center at positive potentials in both dichloromethane and acetonitrile (Table VI). As expected, the 3,5-dimethyl analogues are oxidized at lower potentials than the unsubstituted complexes due to the effect of the electron-releasing methyl groups. Although the redox processes generally appeared to be reversible on the cyclic voltammetric time scale (i.e. ΔE_p nearly independent of scan rate and $i_{pa}/i_{pc} \sim 1$), they were generally irreversible upon bulk electrolysis. One exception, previously reported,[2] is the bulk oxidation of the 3,5-dimethyl(acac) complex, VI, which results in a color change from very pale blue to the deep blue of the monooxo V(V) acac species. This species can be reversibly reduced at 0.0 V if undertaken quickly. If the dark blue species is allowed to stand, the color fades over time to a yellow material which displays completely irreversible electrochemistry. In the case of the unsubstituted complex, bulk oxidation in CH$_2$Cl$_2$ produces a deep violet color only visible right at the electrode surface and which dissipates virtually instantly, producing a red-brown solution. With further aging the solution turns yellow. The final oxidized product cannot be rereduced by electrolysis at 0.0 V and displays completely irreversible electrochemistry. Thus only the 3,5-dimethyl complex sufficiently blocks access to the oxophilic metal center to stabilize the monooxo V(V) complex from further reaction (probably hydrolysis), which produces more stable dioxo V(V) or oxo-bridged V(V) centers.

The LVO(Cl)DMF complexes exhibit similar behavior. Thus oxidation of the 3,5-dimethyl derivative in CH$_2$Cl$_2$ again produces a semistable deep blue monooxo V(V) species whose cyclic voltammogram is identical to that of the starting material. If undertaken quickly, the oxidized complex can be reversibly rereduced at 0.0 V to regenerate starting material. In light of the reversibility evident in the electrochemical oxidation of VIII to its vanadium(V) analogue, it is probably safe to assume that no substantial structural changes accompany this initial redox change. Hence the known structure of the vanadyl starting complex should be a good model for the monooxo V(V) product.[1] The blue monooxo V(V) complex is not highly stable, however, and aging for a period of time results in a color change from blue to yellow with concomitant loss of reversible electrochemistry. Again bulk oxidation of the unsubstituted derivative does not produce the deep blue monooxo V(V) intermediate but rather goes directly to the yellow irreversible product. It is believed that the final yellow product seen with all the complexes upon oxidation represents either dioxo or oxo-bridged V(V) complexes whose formation via hydrolysis could be written as

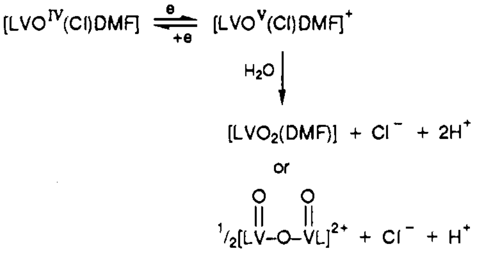

The formation of hydronium ion (H$^+$) in solution is confirmed by the appearance of an irreversible wave at ca. −0.53 V.

The dark blue color of the monooxo V(V) complex of VIII was, in many ways, surprising. While it is well known that monooxo V(V) complexes containing good π-donating oxygen ligands such as the phenolate group display intense LMCT transitions in their optical spectra resulting in deep blue to violet colors, VIII does not contain such a group.[2,12,21] Nevertheless, the intensity of the optical band at 570 nm, ϵ = 1200 M^{-1} cm^{-1}, and the lack of any d electrons in V(V) strongly suggest a LMCT origin. The only potential π donor is the coordinated chloride. This observation may have important implications concerning the binding site in the V(V) dependent enzyme bromoperoxidase where a monooxo V(V) center has been postulated to occur on the basis of EXAFS data and to which halide ion, as a substrate, is assumed to bind.[22,23]

The vanadium(III) complexes III and IV also undergo reversible oxidations as determined by cyclic voltammetry. However, these cyclic voltammograms displayed rather unusual solvent-dependent changes. In dichloromethane, a single quasireversible wave is observed at +1.35 and +1.19 V for III and IV, respectively, while in acetonitrile two distinct redox waves are observed in the same potential range (see Table VI), both of which appear to be quasireversible. Potential cycling through both waves causes a reduction in the magnitude of the first wave with a concomitant growth in the second (Figure 2). Eventually, only a single wave at the higher potential is seen. If, however, the electrolyte solution is extensively degassed (1 h of bubbling with Ar) prior to introduction of either III or IV, then only the lower potential wave is seen. Potential cycling again causes it to diminish in intensity with the growth of the high potential wave. We believe that this curious behavior can be explained by changes in solution occurring at the vanadium center. We propose that the lower potential wave represents the simple one-electron oxidation/reduction, LV^{III}Cl$_2$DMF $\rightleftharpoons$ [LV^{IV}Cl$_2$DMF]$^+$, and the higher potential wave represents the oxidation/reduction of LV^{III}Cl$_2$(ACN) $\rightleftharpoons$

$[LVI^{IV}Cl_2(ACN)]^+$. The acetonitrile adducts are formed by simple solvation:

$$LV^{IV}Cl_2(DMF) + ACN \rightleftharpoons LV^{IV}Cl_2(ACN) + DMF$$

We propose further that the solvation either occurs only in the V(IV) oxidation state or, more likely, is catalyzed by traces of V(IV). Thus under rigorously degassed conditions no electrochemistry attributable to the acetonitrile adduct is observable *until* potential cycling produces some V(IV) to catalyze the solvation. Continued potential cycling allows the solvation to go to completion, and eventually only the electrochemistry attributable to the acetonitrile adduct is seen. In dichloromethane no solvation is seen or expected given the poor ligating ability of that solvent. Identification of the low potential wave with the DMF complex and the high potential wave with the acetonitrile species is consistent with the greater ability of DMF vis-a-vis ACN to stabilize the oxophilic V(IV) center, which allows oxidation to occur at a lower potential. It should be noted that the 3,5-dimethyl derivative has a markedly reduced tendency to undergo the solvation reaction and even after extended potential cycling some of the DMF species is observed. This is again consistent with the more sterically crowded dimethyl derivative protecting the vanadium center from chemical reaction.

Bulk electrolyses on either III or IV are *not* reversible and produce either a yellow material in the case of III or a red-brown product that gradually turns yellow for IV. These products appear to be similar to what were seen with the V(IV) complexes VII and VIII. When these electrolyses are performed at +1.5 V in CH_2Cl_2, two electrons per mole rather than one are removed, indicating ultimate oxidation of V(III) to V(V) on the bulk time scale. That chemical reactions accompany these bulk oxidations is evident from the nonexponential shape of the current vs time plots.

It is somewhat surprising to find the reversible one-electron oxidation of the V(III) species to V(IV) even on the cyclic voltammetric time scale as such oxidations typically produce oxovanadium(IV), i.e., vanadyl, complexes. Since this involves a chemical change (oxo ligand gain or loss) as well as an electron transfer, the cyclic voltammetry is typically irreversible.[24-26] The reversibility seen with III and IV strongly suggests initial oxidation to a non-oxo or bare V(IV) species. However, on the bulk electrolysis time scale, the very oxophilic bare V(IV) species formed has time to react with traces of water and undergo hydrolysis to a vanadyl complex. This, in turn, has an oxidation potential lower than the initial V(III)/V(IV) couple (Table VI) and hence is further oxidized to V(V), an overall two-electron process, i.e.

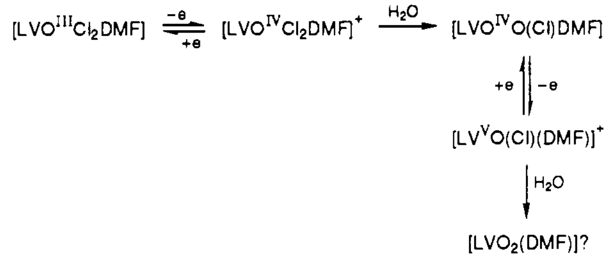

The nature of the final product is, of course, speculative but is consistent with the formation of H^+ seen in the cyclic voltammograms of the electrolyzed material and with known vanadium chemistry.[21]

Finally when the two chlorides and the DMF in III and IV are replaced with another tris(pyrazolyl)borate unit to form the "sandwich" complexes $[L_2V]^+$, the V(III) oxidation state is greatly stabilized. This stabilization is evident from the electrochemistry in that there are no oxidative processes observable out to +2.0 V; rather a facile *reduction* of the V(III) to V(II) is observed in acetonitrile at −0.69 V for I and −0.24 V for II. As expected, the 3,5-dimethyl derivatives, while easier to oxidize, are harder to reduce than their unsubstituted counterparts. The reductions of I and II are completely reversible not only on the CV time scale but on bulk electrolysis as well. Thus, controlled potential electrolysis in either acetonitrile or dichloromethane consumes one electron in both compounds I and II. Reoxidation of the reduced solution at 0.0 V restores the original color, and the solution has an optical spectrum identical with that of the original solution. This process can be repeated many times without evident degradation. Obviously the V(III) and V(II) are tightly encapsulated and thus protected from oxidative or hydrolytic reactions. The stabilization of these lower oxidation states upon replacing the harder chloride and DMF oxygen ligands with the softer nitrogens of another tris(pyrazolyl)borate is consistent with hard/soft acid–base theory.

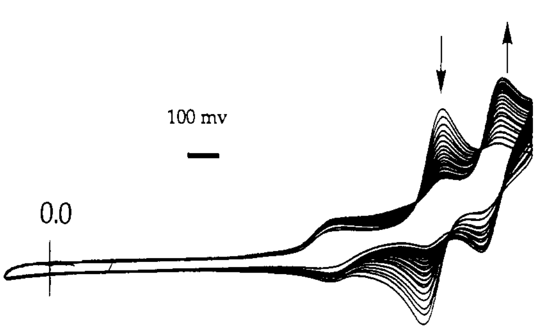

Figure 2. Results of potential cycling between −0.15 and +1.6 V at a 100 mV/s of a solution of $[[HB(pz)_3]VCl_2DMF]$ in acetonitrile. The wave at ~+0.95 V is an impurity in the acetonitrile.

Conclusions. The primary goal of this work was to determine how varying the steric character of ligands coordinated to vanadium(III) or -(IV) complexes of the general type LV(XYZ) affects structural and/or physicochemical properties. These effects were probed by comparing analogous complexes where L is unsubstituted or 3,5-dimethyl-substituted hydridotris(pyrazolyl)borate. In the two cases examined here, no structural effects were evident on changing from the unsubstituted to the (3,5-dimethylpyrazolyl)borate ligand, and only modest and expected changes in ESR or ligand field parameters were detected. These are attributed to the electron-releasing nature of the methyl groups rather than to their steric bulk. The primary differences found appear to be in their kinetic stabilities as manifested in their differing electrochemistry. Substitution of CH_3 for H at the 3,5-positions clearly reduces the accessibility of the metal center and hence confers a measure of kinetic inertness. However, substitution by more sterically demanding groups appears to prevent the formation of stable tris(pyrazolyl)borate complexes. The reasons for this remain unclear and are the subject of further investigations. The presence of a strong LMCT in the monooxo V(V) complex $[LVO(Cl)DMF]^+$ brings into question the direct bonding of halide to the purported monooxo V(V) center in the enzyme bromoperoxidase.

Acknowledgment. This work was supported part by Robert A. Welch Foundation Grant AI-1137 to C.J.C. J.P.J. acknowledges NSF-RUI Instrumentation Grant No. 8818307 for establishment of the New England Molecular Structure Center.

Supplementary Material Available: Tables of complete crystallographic data, fractional atomic coordinates, complete bond distances and angles, and anisotropic thermal parameters (17 pages); a listing of observed and calculated structure factors (48 pages). Ordering information is given on any current masthead page.